

Topologically trapped vortex molecules in Bose-Einstein condensates

R. Geurts,¹ M. V. Milošević,^{1,2} and F. M. Peeters¹,¹Department of Physics, Universiteit Antwerpen, Groenenborgerlaan 171, B-2020 Antwerpen, Belgium²Department of Physics, University of Bath, Claverton Down, Bath, BA2 7AY, UK

(Dated: February 20, 2024)

In a numerical experiment based on Gross-Pitaevskii formalism, we demonstrate unique topological quantum coherence in optically trapped Bose-Einstein condensates (BECs). Exploring the fact that vortices in rotating BEC can be pinned by a geometric arrangement of laser beams, we show the parameter range in which vortex-antivortex molecules or multi-quantum vortices are formed as a consequence of the optically imposed symmetry. Being low-energy states, we discuss the conditions for spontaneous nucleation of these unique molecules and their direct experimental observation, and provoke the potential use of the phase print of an antivortex or a multi-quantum vortex when realized in unconventional circumstances.

PACS numbers: 03.75.Lm, 67.85.Hj, 47.32.cd

During the last decade, intense experimental and theoretical activity has induced dramatic achievements in Bose-Einstein condensation in trapped alkali metal gases at ultralow temperatures [1]. The atomic Bose-Einstein condensates (BECs) differ fundamentally from the helium BEC, having significantly non-uniform density, very high low-temperature condensate fraction, and being pure and dilute, so that interactions can be accurately parametrized in terms of the scattering length. As a result, a relatively simple nonlinear Schrödinger equation (the Gross-Pitaevskii (GP) equation) gives a precise description of the atomic condensates and their dynamics [2].

It is already well established that the GP equation has rotating solutions with a well-defined angular momentum, defining the vortex states [3]. Vortices as topological singularities in BEC have been readily observed in experiment [4], and are also found in liquid helium [5] and in superconductors [6]. The exciting new property of atomic BECs is that intrinsic interactions in the system are directly dependent on the mean particle density [7], which gives them a unique degree of freedom for studies of vortex matter. Another interesting aspect of dilute Bose condensates is that their density can be locally suppressed optically. As experimentally shown by Tung et al. [8], vortex lines in BEC show great affinity towards weak spots created by focussed laser beams, which results in a very profound vortex pinning and provides yet another tool for vortex manipulation [9].

Vortices in BEC are accompanied by the appropriate distribution of the phase θ of the order parameter ψ , where the number of successive 2π changes along the perimeter corresponds to the vorticity of the vortex state, i.e. the topological charge. Therefore, using the known phase distribution, particular vortex states can be predefined in the system by the so-called phase imprint technique [10], where an uniform light pulse projects a designed mask onto the condensate. However, the gradient of the imprinted phase ($\nabla\theta$) must always be parallel to

the rotational velocity of the condensate, i.e. the antivortex is fundamentally unstable for a positive angular momentum. Note also that imprinted multiple 2π change, i.e. a multi-quantum vortex, was never found stable against decomposition into single vortices in conventional BEC setups [11].

Motivated by these recent developments in vortex physics, in this paper we exploit a uniquely defined BEC system that combines above essentials; our atomic BEC is confined, exposed to engineered spatial pinning, and is cylindrically rotated. Knowing that vortex solitons are strongly influenced by symmetry in non-linear media [12], we impose a particular symmetry on the system by chosen arrangement of the vortex-trapping optical beams. As we will show, this results in the nucleation of vortex molecules of matching symmetry in the ground state, which may comprise unconventional phase profiles containing a stable antivortex, or a multi-quantum vortex.

For the purpose of this work, we solve the stationary Gross-Pitaevskii (GP) equation, in a rotating frame with frequency ω around the z-axis:

$$-\frac{\hbar^2}{2m} \nabla^2 \psi + V_c + g|\psi|^2 \psi - i\hbar \omega L_z \psi = 0; \quad (1)$$

where V_c stands for confinement potential, $g = 4\pi\hbar^2 a/m$ is the non-linearity with a being the s-wave scattering length, $L_z = i\hbar(x\partial_y - y\partial_x)$ is the angular momentum operator, μ denotes chemical potential, and ω is the order parameter normalized to the number of particles in the condensate N . The energy of a particular state is then given by $E = \frac{g}{2} \int dV |\psi|^4$. We take the usual parabolic-like confinement potential characterized by the frequency ω_\perp in the (x,y) plane and ω_z in the z -direction. Our numerical method treats the GP equation in all three dimensions, but in the present work we take $\omega_z \rightarrow 0$, forcing the condensate in a quasi-two-dimensional, oblate (pancake) shape. In that case, Eq. (1) can be written in dimensionless and discretized form as

$$\frac{U_x^{i-1,j;i-1,j}}{b_x^2} + \frac{U_x^{i+1,j;i+1,j}}{b_x^2} + \frac{U_y^{j-1,i;j-1,i}}{b_y^2} + \frac{U_y^{j+1,i;j+1,i}}{b_y^2} = \frac{2}{b_x^2} + \frac{2}{b_y^2} g' j_{ij} j_{ij} V + \dots \quad (2)$$

where $b_{x,y}$ are the lattice constants of the Cartesian grid, and the link variable is defined as $U_{x,y}^{m,n} = \exp \left(i \int_{x_m}^{x_n} A(x) dx \right)$, with $A_x(y) = \left(\frac{1}{2} \right) y(x)$. The distances, angular velocity and energy are expressed in the fundamental scales of the harmonic trap, i.e. $r_0 = \sqrt{\hbar / m \omega_z}$, $\omega_z = \omega_z$, and $E_0 = \hbar \omega_z$ respectively. The 2D nonlinearity $g^0 = 2a N \omega_z \sim \omega_z$ (found by averaging the GP equation over the z -direction) now depends on N since we chose wave function normalized to unity. Therefore, for fixed g , N is a measure of the importance of interactions in the condensate, and directly reflects on the vortex phase diagram. Note also that for low non-linearities, i.e. when g' is small, vortex states in parabolic confinement are stable only for velocities of the condensate close to ω_z , i.e. when the gas dissolves due to centrifugal forces. To enhance the vortex stability, we have chosen a modified confinement potential $V_c = \frac{1}{2} r_z^2 + \frac{1}{10} r_z^4$. Such empowered confinement enables the condensate to survive higher angular velocities ($> \omega_z$), and is feasible in experiment by combining optical and magnetic trapping (e.g. for ^{87}Rb , a magnetic trap with frequency 75.5×10^3 Hz in combination with a laser beam with waist $25 \mu\text{m}$ and power 1.2 mW [13]).

Vortex-antivortex molecules as the ground state. In this paper, we consider ^{23}Na BEC, with somewhat lower interaction than ^{87}Rb , and consequently lower non-linearity. With the above expression for V_c , we use the effective perpendicular parabolic confinement with $\omega_z = 4.39 \times 10^3$ Hz, and the unit of length becomes $r_0 = 10 \mu\text{m}$. To obtain the pancake shape of the condensate, we take $\omega_z = 10 \omega_z$. The non-linearity parameter for a condensate consisting of 10^4 sodium atoms becomes $g^0 = 44$. In what follows, we implement laser pinning in the formalism, and model it as a Gaussian potential well $V_p = \exp(-16(r-w_p)^2)$ (r is the distance from the pinning center) as depicted schematically in the inset of Fig. 1c. We use a set of N_p laser beams on a single ring, and compare first the energy in the absence and presence of pinning, as shown in Fig. 1c. The resulting total potential in the BEC, introduced by confinement and laser beam s , is taken as

$$V = V_c(\mathbf{r}) + \sum_{j=1}^{N_p} V_p(\mathbf{r} - \mathbf{r}_j)$$

with $\mathbf{r}_j = d_p [\cos(j/2 - N_p) \mathbf{e}_x + \sin(j/2 - N_p) \mathbf{e}_y]$. With increasing angular velocity $\omega_z = \omega_z$, vortices stabilize in the system, and each vortex state exhibits a distinct energy. In the $N_p = 0$ case, for chosen param-

eters, individual vortices form multi-vortex patterns denoted by $(L_c; L)$, where L_c gives the number of vortices in the central part of the condensate i.e. $L_c = \lim_{\omega_z \rightarrow 0} \frac{1}{2\pi} \oint \mathbf{r} \cdot d\mathbf{r}$, and L is the total vorticity. In the $N_p \neq 0$ case, the ordering of laser beams imposes its symmetry on the vortex states, with N_p vortices pinned by the laser beams, and the remaining ones sitting in the central region of the condensate. As a remarkable phenomenon, the system may preserve the symmetry even for $L < N_p$; e.g. for $L = N_p - 1$, still N_p vortices nucleate and are pinned, but must be accompanied by a central antivortex in order to simultaneously match the total angular momentum and the symmetry of the pinning potential. Energy levels of such vortex-antivortex molecules are indicated in Fig. 1 for $N_p = 3$ and $N_p = 5$ by the dotted (blue) curves.

Vortex-antivortex (V-Av) phenomena has already been of interest in BEC, mainly due to the fact that the excitation energy of a vortex-antivortex pair in non-rotating condensate is lower than the one of a single vortex. For

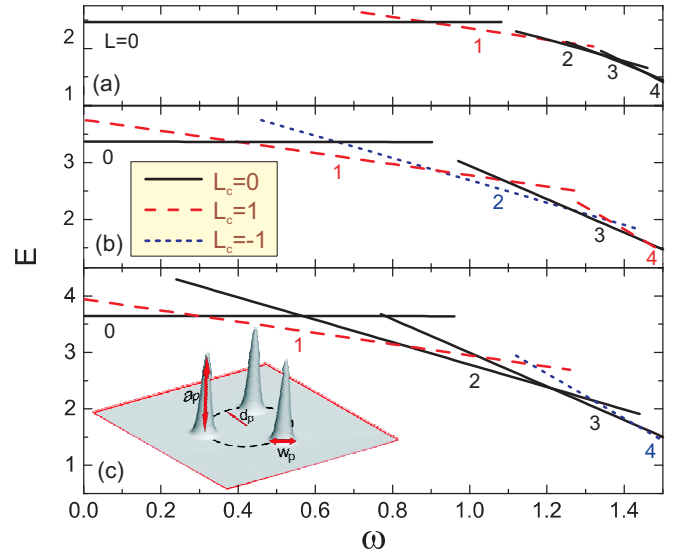


FIG. 1: (Color online) Energy versus angular velocity of a ^{23}Na condensate with $g' = 20$ (i.e. with $N = 5000$ atoms), in the case of no laser pinning ($N_p = 0$, a), and three ($N_p = 3$, b), and five ($N_p = 5$, c) laser beams in a polygonal setting (with $d_p = 0.5$, $w_p = 0.4$, $a_p = 500$). Different lines correspond to states with different total vorticity L . The colors and style of the lines indicate the vorticity in the center of the condensate (L_c). The inset depicts the used energy profile for each pinning site, and notation of the parameters.

that reason, it was assumed that the actual nucleation of a vortex occurs through the generation of a V-Av pair and the subsequent expulsion of the antivortex [14]. While this may hold in ideally non-interacting BEC, V-Av appearance is seriously hampered by even small perturbations in the system, particularly in the rotating one. Yet, Crasovan et al. demonstrated that a V-Av pair may be stable in an interacting non-rotating BEC, however only as an excited state (ground state remains vortex-free) [15] and the dynamics of such a state was recently analyzed in Ref. [16]. In addition, vortex-antivortex clusters were studied in Ref. [17], the stabilization of vortex-antivortex lattices was considered in Ref. [18] and a superposed vortex-antivortex state was investigated in Ref. [19], however all only for the case of non-rotating systems. Here we show that states comprising an antivortex can be stabilized as the ground state in a rotating BEC by engineered pinning. Moreover, by using a different number of laser beams, antivortex can be realized at different angular velocities. Fig. 2 shows the ω -stability range of V-Av states with one antivortex found for $N_p = 3 - 7$, thus all states having vorticity $L = N_p - 1$. With increasing N_p , not only V-Av states appear for higher angular momenta, but they can also be spread over a larger area of the condensate. When artificially spreading the laser beams further apart (increasing d_p , see Fig. 1), vortices spontaneously follow and increase their distance from the central antivortex (d_{av}) which facilitates the experimental verification of the V-Av molecule. Fig. 2 also shows the maximal d_{av} that can be reached by increasing d_p for $w_p = 0.5$, $a_p = 500$ and $g^0 = 40$. The insets of Fig. 2

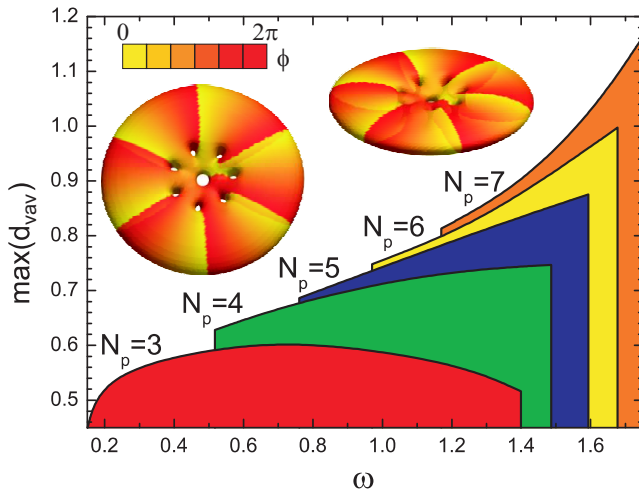


FIG. 2: (Color online) Histogram of vortex-antivortex (V-Av) distance in stable molecules found for different number of equidistant laser beams on a ring, as a function of angular velocity for $g^0 = 40$. Maximal V-Av separation increases for more used pinning beams, and insets show two oblique views of the superimposed density/phase 3D plots of the condensate for $\omega = 1.71$ and $N_p = 7$.

show isosurfaces of density 10^{-6} on which the phase distribution is superimposed for a condensate in the V-Av state for $N_p = 7$, $g^0 = 22$ and $\omega = 1.71$.

Novel phase transitions. As much as V-Av states are novel and exciting study objects, our system actually exhibits even richer vortex structures beyond V-Av phenomena. To illustrate this, we constructed a full vortex phase diagram, shown in Fig. 3 as a function of ω and non-linearity g^0 , for $N_p = 4$, i.e. a square arrangement of laser beams. As shown before, for constant g^0 , the vorticity increases with increasing ω . Note however that our strategic pinning setup enforces the N_p -fold symmetry of the vortex states, which leads to specific transitions in the central region of the condensate. As illustrated by a color gradient in Fig. 3, the central vorticity changes as $L_c = \text{mod}(\omega + 1; N_p) - 1$, where an antivortex may nucleate as discussed above. Nevertheless, N_p -fold symmetry tends to remain preserved for other vorticities as well, which results in the compression of excess $L - kN_p$ ($k \in \mathbb{Z}$) vortices in the center of the condensate into a multi-quantum vortex (also called giant vortex). This result complements earlier studies of such vortices in conventional BEC setups, where a multi-quantum vortex was found unstable towards decay into single-quantum vor-

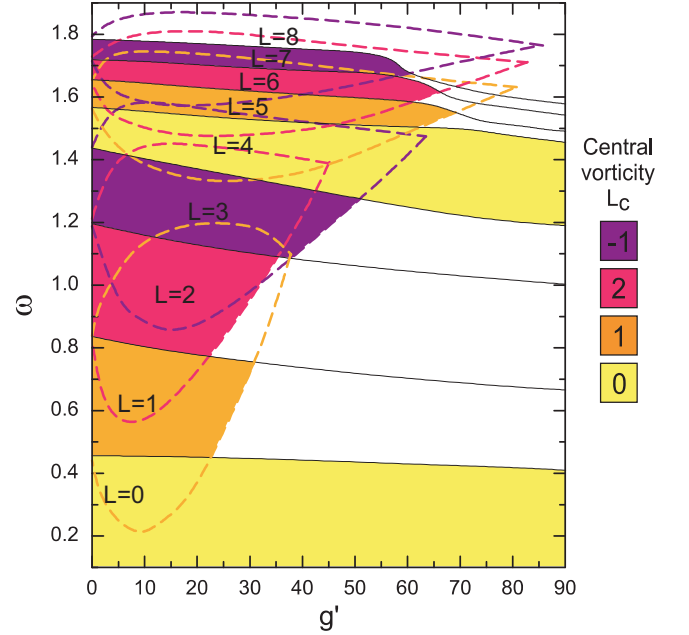


FIG. 3: (Color online) Equilibrium vortex phase diagram as a function of the angular velocity and non-linearity of the condensate, for $N_p = 4$, $d_p = 0.71$, $w_p = 0.4$ and $a_p = 500$. Coloring scheme illuminates the vorticity in the center of the condensate, between the pinning beams. Solid lines show the transitions in the ground state, while dashed curves illustrate the whole region of stability for different vortex states. In white areas, the vortex structure does not fully obey the four-fold symmetry of the pinning.

tices [11]. For $N_p = 4$, we show the $0;1;2; \dots; 1;0;1;2; \dots; 1$ sequence with increasing l in Fig. 3, for total vorticity $L = 0 \dots 7$. Doubly quantized vortex was realized for $L = 2$ and $L = 6$ states in the center of the condensate.

While the existence of stable multiquantum vortices was already predicted in several theoretical papers for condensates in a confinement potential with a quartic component [20], our giant vortices are solely a consequence of the symmetry induced by the pinning centers, as can be deduced from Fig. 4(d) for the $L = 6 = 4 + 2$ state: The giant vortex state is not stable when w_p is too small. By doing two separate simulations of a condensate in conventional parabolic confinement – thus without quartic component – exposed to 4 pinning beams, we were able to confirm this statement: We found a giant vortex in both the ground states for $L = 2$ (with $g = 20$, $l = 0.85$, $d_p = 0.8$, $w_p = 0.6$, $a_p = 50$) and $L = 6 = 4 + 2$ ($g = 40$, $l = 0.85$, $d_p = 1.3$, $w_p = 1.6$, $a_p = 200$). This general behavior holds for arbitrary number of pinning beams. In other words, vortex molecules comprising multiquantum vortices are stable in our system, contrary to conventional behavior of BEC. Moreover, we report here a unique way of engineering locally the phase imprint of the condensate, by either changing angular velocity, or the non-linearity (e.g. by condensing more constituent atoms). The limits of this procedure are: (i) the deconfinement of the condensate at large l , and (ii) the maxi-

mal g^0 at which vortex-vortex interaction overwhelms the optical pinning, resulting in a vortex structure that does not fully obey the imposed geometry (white areas in Fig. 3).

Stability and control of special vortex states. Obviously, the exact parameters of the strategically placed laser beams are very deterministic for the resulting vortex structure in the condensate. Here we briefly discuss the influence of beam intensity, distance between adjacent beams, and their focussed waist on V-Av and multiquantum states. Our results are summarized in Fig. 4. Figs. (a)–(c) relate to V-Av molecules in fourfold pinning, and help visualize their stability and size in a two-parameter space. As a general conclusion, we find that a larger amplitude of the pinning (a_p , see inset of Fig. 1) is always beneficial to the V-Av state. Simply, stronger imposed pinning reflects better its symmetry on the vortex state. For the same reason, strong overlap between pinning profiles of the beams should be avoided (i.e. $w_p \lesssim 3d_p$ is desirable). As shown in Fig. 4, the distance between the central antivortex and pinning vortices can be increased by increasing the spacing between the beams (d_p); this is nevertheless a limited option, as vortices may not follow the imposed pinning at large distances from the center of the condensate. For considered parameters, we realized maximal V-Av distance of approximately $0.9r_0$, which is of the order of 10 nm for the sodium condensate, and thus feasible for experimental observation. The used beam width of $w_p = 0.2 \dots 1.5r_0$ and sub- r_0 distances for beam ordering are also very realistic values for the available experimental techniques.

Fig. 4(d) shows the stability region of a doubly quantized vortex in a fourfold geometry of the $L = 6$ state ($4 + 2$). Similarly to the V-Av case, imposed symmetry of the pinning is essential for the nucleation of the double vortex. Relatively weaker pinning by wider laser beams can significantly enhance the stability of the multiquantum vortex, while the clarity of its separation from the surrounding vortices is best achieved for high beam amplitudes and narrow beam waists. However, the needed d_p is quite low, as confinement between the pinning beams must remain firm for the stabilization of the multiquantum vortex. Such small spacing is unfavorable for experimental observation, but can be significantly improved in the case of larger N_p and larger vorticity. This analysis and the complete investigation of all stable vortex states in this phenomenologically rich system will be presented elsewhere.

Fig. 4(d) shows the stability region of a doubly quantized vortex in a fourfold geometry of the $L = 6$ state ($4 + 2$). Similarly to the V-Av case, imposed symmetry of the pinning is essential for the nucleation of the double vortex. Relatively weaker pinning by wider laser beams can significantly enhance the stability of the multiquantum vortex, while the clarity of its separation from the surrounding vortices is best achieved for high beam amplitudes and narrow beam waists. However, the needed d_p is quite low, as confinement between the pinning beams must remain firm for the stabilization of the multiquantum vortex. Such small spacing is unfavorable for experimental observation, but can be significantly improved in the case of larger N_p and larger vorticity. This analysis and the complete investigation of all stable vortex states in this phenomenologically rich system will be presented elsewhere.

Conclusions. In summary, using a novel concept of polygonal optical pinning, we demonstrated yet unpredicted vortex states in rotating atomic Bose-Einstein condensates. We realized a stable antivortex for positive angular momentum, as well as a multiquantum vortex, which up to now was assumed to be unstable in BEC. Both are found as the ground state for a wide range of parameters. New ground-state transitions found by in-

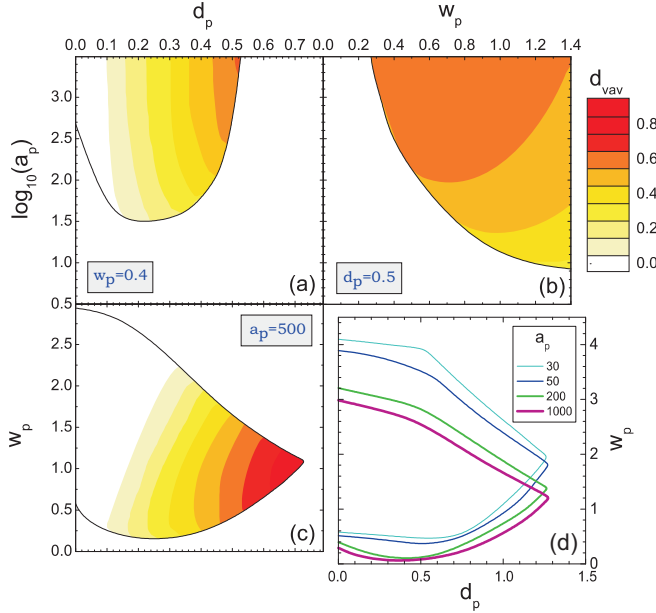


FIG. 4: (Color online) Influence of the optical parameters of the laser beams on the stability of the special vortex molecules found for $N_p = 4$. (a–c) V-Av stability and spacing in a two-parameter space, thus for either fixed amplitude, separation, or focused width of the beams ($g^0 = 40$, $l = 1.25$). (d) The stability region of the doubly quantized vortex in the center of a $L = 6$ state, for different values of a_p ($g^0 = 40$, $l = 1.6$).

